Reactions of Laser-Ablated Boron Atoms with Methyl Halides in Excess Argon. Infrared Spectra and Density Functional Theory Calculations on CH_3BX, CH_2BX, and CHBX (X = F,Cl,Br)

Dominick V. Lanzisera† and Lester Andrews*

Department of Chemistry, University of Virginia, Charlottesville, Virginia 22904-4319

Received: May 11, 2000; In Final Form: August 3, 2000

Laser-ablated boron atoms react with methyl fluoride in an argon stream to form two major products: CH_2-BF and CHBF. In similar reactions of boron with methyl chloride and methyl bromide, both CH_2BX and CHBX are also observed, as well as the primary insertion products, CH_3BCl and CH_3BBr, respectively. Infrared spectra of isotopic combinations of B and CH_3X and density functional theory frequency calculations provide evidence for the product identification. Both products form via insertion into the C−X bond followed by loss of one or two H atoms for all reactions. Comparisons are made with the products of the reactions of B with C_2H_6, CH_3NH_2, and CH_3OH, all of which are isoelectronic with CH_3F. The calculations not only predict the vibrational frequencies exceptionally well, but also predict that there is no dative bonding in either CH_2BX or CHBX, despite the empty p-orbital on B and the filled p-orbitals on the halogen atom.

Introduction

Because boron has one fewer electron than carbon, compounds containing boron are relatively unstable compared to their carbon-containing analogues. For this reason, matrix isolation, in which unstable products of reaction are preserved in a cage of an inert solid, has been essential in the study of these boron products.[1] For example, while C_2H_4 is found in nature, similar compounds such as CH_2BH_2, CH_2BH, and CHBH have been characterized only in a matrix in the laboratory.[2]

In previous studies, laser-ablated boron reacted with small gases in excess argon to produce novel products. One series of such experiments involved characterizing the product of boron reactions with C_2H_6,[1] CH_3NH_2,[3] and CH_3OH.[4] These reactants are isoelectronic and, therefore, form similar products. The major products of these reactions formed following insertion into the C−C, C−N, or C−O bond. Elimination of one hydrogen atom typically followed, yielding the major products CH_3BCH_2, CH_3-BNH, and CH_3BO, respectively. Note that for CH_3BNH and CH_3BO, the hydrogen elimination occurs from the more electronegative atom. Other less prominent species were present in each matrix isolation study, but the major products all seemed to result from the same reaction mechanism, yielding a product with a B═C, B═N, or B═O bond. In the last two cases, calculations reveal a formal positive charge on the nitrogen and oxygen atoms due to p-orbital donation from the filled shell to the empty p-orbital of the B atom.

This article presents the conclusion of this series of reactions, the reaction of boron with CH_3X (X = F,Cl,Br), with primary focus on the methyl fluoride experiments. Although CH_3F is isoelectronic with C_2H_6, CH_3NH_2, and CH_3OH, there is no terminal hydrogen atom on the fluoride. Therefore, the mechanism for the major products in this reaction must be different from those of the previously studied reactions.[1−4] It is more likely, then, that the new species would resemble the *minor* products of the ethane, monomethylamine, and methanol reactions. Also, the strongly electronegative fluorine atom tends not to donate its p-orbital electrons as readily as nitrogen and oxygen. This suggests that the chemical nature of the observed products may be quite different from their isoelectronic counterparts in the previously studied reactions.

Experimental Section

The apparatus for pulsed laser ablation, matrix isolation, and infrared spectroscopy has been described previously.[5,6] Mixtures of 0.5% CH_3F, $^{13}CH_3F$, or CD_3F in argon co-deposited at 3 mmol/h for 2 h onto a 6−7 K cesium iodide window react with boron atoms ablated from a target source rotating at 1 rpm. Three samples of boron were employed: neutral isotopic ^{n}B (Aldrich, 80.4% ^{11}B, 19.6% ^{10}B) and ^{10}B (93.8%, Eagle Pitcher, Ind.). Similarly, we used three samples of CH_3F: $^{12}CH_3F$ (Matheson), $^{13}CH_3F$ (MSD Isotopes), and CD_3F (MSD Isotopes). The fundamental 1064 nm beam of a Nd:YAG laser (Spectra Physics DCR-11) operating at 10 Hz and focused with a focal length = +10 cm lens ablated the target using 20 mJ per 10 ns pulse. Following deposition, a Nicolet 550 Fourier transform infrared (FTIR) spectrometer collected infrared spectra from 4000 to 400 cm^{-1} using a liquid-nitrogen-cooled HgCdTe detector; the resolution was 0.5 cm^{-1} with a frequency accuracy of ±0.2 cm^{-1}. After sample deposition, annealing to 15 K followed by broadband (λ > 240 nm) mercury arc photolysis (Philips 175 W) produced changes in the FTIR spectra. Further annealings to 25 and 35 K also changed some of the spectral features.

Experiments with methyl chloride and methyl bromide were conducted similarly for comparison. The boron samples, laser power and repetition rate, gas flow, matrix isolation, and photolysis and annealing cycles were the same as for the methyl fluoride experiments. The samples employed were CH_3Cl (Matheson), CD_3Cl (synthesized using CD_3OD and mesyl chloride), CH_3Br (Matheson), and CD_3Br (MSD Isotopes). In addition, supplemental experiments with CH_2Cl_2 (Fisher, re-

* Author to whom correspondence should be addressed.
† Present address: Jobin Yvon Inc., 3880 Park Ave., Edison, NJ 08820.

10.1021/jp0017689 CCC: $19.00
Published on Web 09/21/2000

TABLE 1: Observed Frequencies (cm^{-1}) for Products from Boron−Methyl Fluoride Reactions

12/1[a]	13/1[a]	12/2[a]	phot/ann[b]	identity
3261.7	3250.0	2468.5	+15/+5	CHBF
3050.2	3044.8		+20/−10	CH_2BF
1884.7	1872.5	1845.3	+15/+5	$CH^{10}BF$
1822.3	1810.8	1786.8	+15/+5	$CH^{11}BF$
1822.0	1816.6	1801.0	+20/−10	$CH_2{}^{10}BF$
1762.2	1751.3	1741.5	+20/−10	$CH_2{}^{11}BF$
919.5	905.5		+20/−10	$CH_2{}^{10}BF$
917.4	905.5		+20/−10	$CH_2{}^{11}BF$
767.5	761.4	687.3	+20/−10	$CH_2{}^{10}BF$
755.0	748.8	671.8	+20/−10	$CH_2{}^{11}BF$
590.2	587.2		+20/−10	$CH_2{}^{10}BF$
589.5	587.0		+20/−10	$CH_2{}^{11}BF$

[a] Isotopes for carbon/hydrogen. [b] Percent increase or decrease on photolysis/annealing to 25 K.

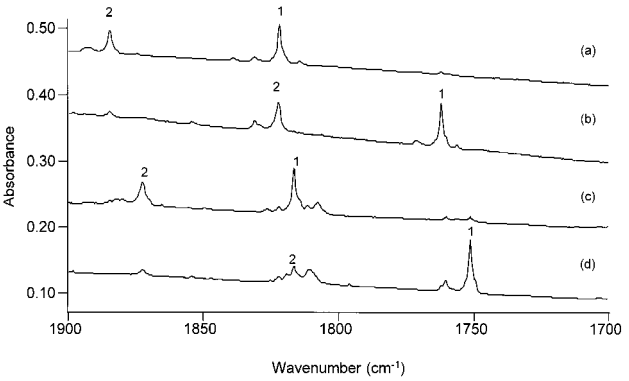

Figure 1. Matrix infrared spectra in the 1900−1700 cm^{-1} B═C stretching region following pulsed laser ablation of B atoms co-deposited with Ar/CH_3F (200:1) samples on a CsI window at 6−7 K. (a) $^{10}B + {}^{12}CH_3F$, (b) $^{n}B + {}^{12}CH_3F$, (c) $^{10}B + {}^{13}CH_3F$, and (d) $^{n}B + {}^{13}CH_3F$.

agent) and $CHCl_3$ (Fisher reagent) were also done under conditions identical to those of the methyl halides.

We perfomed density functional theory (DFT) computations on potential product species using the Gaussian 94 program package.[8] Calculations used the BP86 pure density functional, and the 6-311G* basis set for each atom with one single first polarization function.[9,10] The geometries were fully optimized, and the frequencies were calculated analytically. Experience has shown that BP86 calculations predict vibrational frequencies with good accuracy.[11−14]

Results

Matrix infrared spectra for several isotopic combinations are reported as well as the relative change in intensity of product bands following mercury arc photolysis and subsequent annealing to 25 K. The results from annealing to 35 K confirm the assignments made from analyzing the photolysis and 25 K annealing behavior but do not typically provide additional information as to product identification.

B + $^{12}CH_3F$. Table 1 lists all the observed frequencies as well as the photolysis and 25 K annealing behavior for all product bands. In Figure 1, a and b represent the spectrum in the 1900−1700 cm^{-1} range for reactions of ^{10}B and ^{n}B, respectively, with $^{12}CH_3F$. This frequency range represents the B═C stretching region. The strongest absorption in Figure 1b, labeled 1, at 1762.2 cm^{-1} has a ^{10}B counterpart at 1822.0 cm^{-1}. These bands increase 20% on photolysis and decrease 10% on annealing. In the ^{n}B spectrum, this band is obscured by a stronger band at 1822.3 cm^{-1}, which increases 15% on photolysis and increases 5% on annealing. This band is also nearly as intense as the 1762.2 cm^{-1} band, and is therefore of a different product. This second peak, labeled 2, has a ^{10}B counterpart in Figure 1a at 1884.7 cm^{-1}.

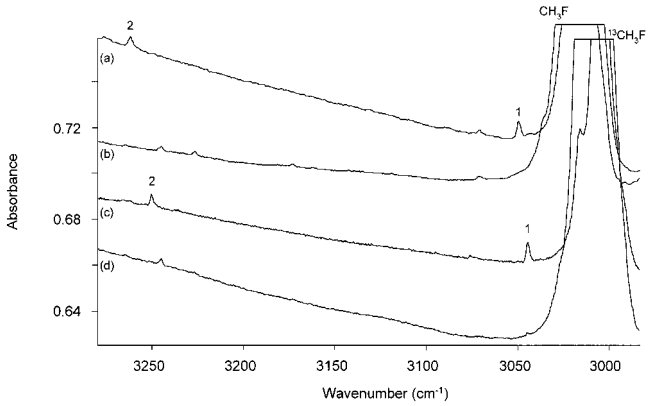

Figure 2. Matrix infrared spectra in the 3290−2980 cm^{-1} C−H stretching region following pulsed laser ablation of B or Be atoms co-deposited with Ar/CH_3F (200:1) samples on a CsI window at 6−7 K. (a) $^{n}B + {}^{12}CH_3F$, (b) Be + $^{12}CH_3F$, (c) $^{n}B + {}^{13}CH_3F$, and (d) Be + $^{13}CH_3F$.

In the C−H stretching region (Figure 2a), most bands are provided by CH_3F precursor and photofragments from the ablation reactions. These bands also appear in an FTIR spectrum following reaction of Be with CH_3F (Figure 2b),[15] indicating that these products do not contain boron or beryllium. Two weak bands, however, are unique to the boron results, at 3050.2 and 3261.7 cm^{-1}; neither band shows any boron isotopic shift. The 3050.2 cm^{-1} peak has photolysis and annealing behavior similar to that of the product labeled 1 in Figure 1, while the 3261.7 cm^{-1} band tracks with the product labeled 2.

There are other, weaker bands in the lower energy region. A peak tracks with product 1 at 919.5 cm^{-1} for ^{10}B with a ^{11}B counterpart at 917.4 cm^{-1}. Both bands increase 20% on photolysis and decrease on annealing. In the expected C−F and B−F regions of the spectrum, a peak with an appreciable boron shift has frequencies at 767.5 and 755.0 cm^{-1} for ^{10}B and ^{11}B, respectively, while in the bending region another peak shows a smaller boron shift at 590.2 and 589.5 cm^{-1}.

B + $^{13}CH_3F$. In Figure 1, c and d are the spectra for the reaction products of ^{10}B and ^{n}B, respectively, with $^{13}CH_3F$ in the B═C stretching region. As with the $^{12}CH_3F$ spectra, there are two major bands each in this region. The stronger band, labeled 1, has a ^{11}B component at 1751.3 cm^{-1} and tracks with the Figure 1b spectrum peak at 1762.2 cm^{-1}. The ^{10}B counterpart at much higher frequency, 1816.6 cm^{-1}, shows the expected 1:4 ratio in intensity with the 1751.3 cm^{-1} peak in the ^{n}B spectrum. As with the ^{12}C results, there is a less intense band at higher energy. This second peak, at 1810.8 and 1872.5 cm^{-1}, increases on both photolysis and annealing, and thus tracks with product 2.

Figure 2c shows the $^{13}C-H$ stretching region for the boron reaction, while Figure 2d shows the analogous beryllium reaction. As with ^{12}C, there are two bands unique to the boron reaction that exhibit a carbon isotopic shift, but no such shift for boron substitution. These bands also track with their counterparts from Figure 2a. The peak for product 1 is at 3044.8 cm^{-1}, while the peak for product 2 is appreciably higher in frequency at 3250.0 cm^{-1}.

For the lower bands, product 1 absorbs at 905.5 cm^{-1} with no boron shift and at 748.8 and 761.4 cm^{-1} for ^{11}B and ^{10}B, respectively. In the bending region, boron isotopic bands appear at 587.0 and 587.2 cm^{-1}.

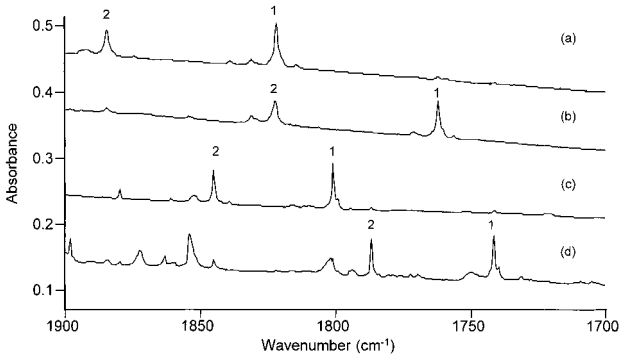

Figure 3. Matrix infrared spectra in the 1900−1700 cm^{-1} B═C stretching region following pulsed laser ablation of B atoms co-deposited with Ar/CH_3F (200:1) samples on a CsI window at 6−7 K. (a) $^{10}B + {}^{12}CH_3F$, (b) $^{n}B + {}^{12}CH_3F$, (c) $^{10}B + {}^{12}CD_3F$, and (d) $^{n}B + {}^{12}CD_3F$.

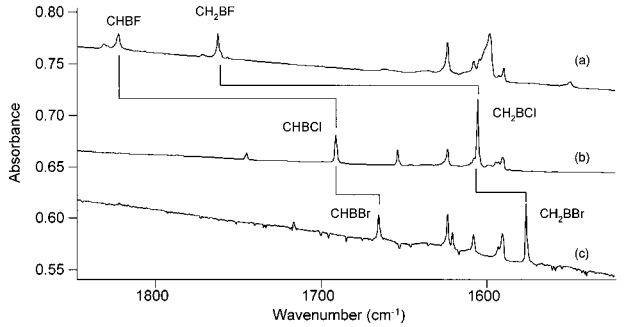

Figure 4. Matrix infrared spectra in the 1850−1500 cm^{-1} B═C stretching region following pulsed laser ablation of B atoms co-deposited with Ar/CH_3X (200:1) samples on a CsI window at 6−7 K. (a) $^{n}B + {}^{12}CH_3F$, (b) $^{n}B + CH_3Cl$, and (c) $^{n}B + CH_3Br$.

B + $^{12}CD_3F$. Figure 3a−d presents the spectra in the B═C stretching region for reactions of boron with both CH_3F and CD_3F. Again, there are two main products here, and they both exhibit very large boron isotopic boron shifts. The strongest band in the ^{11}B spectrum (Figure 3d) has a frequency of 1741.5 cm^{-1} and tracks with the 1801.0 cm^{-1} peak from Figure 3c, the ^{10}B spectrum. As with the other isotopes, the relatively minor product is at higher frequency. The 1786.8 and 1845.3 cm^{-1} peaks track with the species 2 bands in the other isotopic experiments.

In the C−D stretching region, only one peak was observed that could be distinguished from CD_3F fragments. A band at 2468.5 cm^{-1} was sufficiently higher in frequency than the fragment peaks and increased on both photolysis and annealing, thus tracking with the 3261.7 cm^{-1} peak in Figure 2a. In the B−F and C−F stretching regions, peaks at 671.8 and 687.3 cm^{-1} for ^{11}B and ^{10}B, respectively, show the same photolysis and annealing behavior as the product labeled 1 in the previous spectra.

B + CH_3Cl. As with the CH_3F reactions, there are some prominent peaks present in the B═C stretching region of the spectrum, but in the CH_3Cl case shifted lower in energy. Figure 4 presents spectra in this region for all of the methyl halide reactions using natural isotopes. Product band assignments will be discussed in the next section. Table 2 lists the observed product bands for both the CH_3Cl and CH_3Br experiments for the various isotopic combinations. For the chloride reactions, two prominent bands in this region arise. The first of these, at 1691.1 and 1744.8 cm^{-1} for ^{11}B and ^{10}B, respectively, increases 35% on photolysis, while the lower frequency peaks (at 1605.7 and 1653.8 cm^{-1}) increase only 15% on photolysis. Both of these bands decrease on annealing. These absorptions have large boron isotopic frequency shifts as in the analogous methyl fluoride experiments. As Table 2 shows, the deuterium shifts for these absorptions are less than the boron shifts, indicating that this mode has relatively high B motion in the vibration with relatively low H atom involvement. These observations indicate that both absorptions are B═C vibrations, but of different products.

TABLE 2: Observed Frequencies (cm^{-1}) for Products from Boron−Methyl Chloride and Boron−Methyl Bromide Reactions

$^{11}B + CH_3X$	$^{10}B + CH_3X$	$^{11}B + CD_3X$	$^{10}B + CD_3X$	phot/ann[a]	identity
3251.2	3252.3	2464.1	2468.6	+35/−15	CHBCl
3248.2	3250.4	2461.9	2465.1	+15/0	CHBBr
3045.1	3045.1	2224.7	2227.2	+15/+15	CH_2BBr
		2232.4	2232.4	+15/−20	CH_2BCl
1691.1	1744.8	1644.3	1696.3	+35/−15	CHBCl
1665.1	1716.6	1616.3	1666.3	+15/0	CHBBr
1605.7	1653.8	1570.3	1625.5	+15/−20	CH_2BCl
1576.0	1620.7	1541.0	1586.6	+15/+15	CH_2BBr
1172.7	1201.2	1161.0	1185.9	−20/+55	CH_3BCl
1178.4	1206.2	1163.8	1188.5	−20/−40	CH_3BCl site
1142.4	1170.5	1161.0	1185.9	−10/+55	CH_3BBr
1147.8	1175.9	1163.8	1188.5	+15/−50	CH_3BBr site
686.9	696.0	611.1	623.4	+15/−20	CH_2BCl

[a] Percent increase or decrease on photolysis/annealing to 25 K.

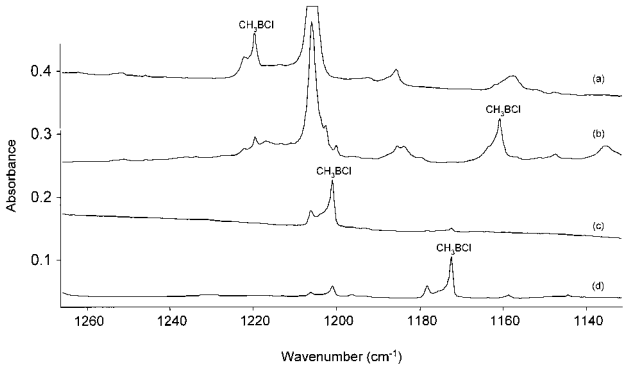

Figure 5. Matrix infrared spectra in the 1270−1130 cm^{-1} B−C stretching region following pulsed laser ablation of B atoms co-deposited with Ar/CH_3Cl (200:1) samples on a CsI window at 6−7 K. (a) $^{10}B + CH_3Cl$, (b) $^{n}B + CH_3Cl$, (c) $^{10}B + CD_3Cl$, and (d) $^{n}B + CD_3Cl$.

Also listed in Table 2 are peaks in the C−H stretching region of the spectrum. Only one such band appears in the CH_3Cl experiments, and this absorption, at 3251.2 and 3252.3 cm^{-1} for ^{11}B and ^{10}B, respectively, track with the 1691.1/1744.8 cm^{-1} bands in the B═C stretching region. The relatively high energy of this band is indicative of a C−H mode with a single hydrogen. With CD_3Cl experiments, two sets of bands appear. One peak at 2464.1/2468.6 cm^{-1} tracks with the C−H peak from the CH_3Cl experiments. Another, at lower frequency, does not have an H atom counterpart. It is likely that such a peak may be obscured by the CH_2Cl photofragment absorption in this region.

In the B−C stretching region, near 1200 cm^{-1}, asymmetric bands appear with isotopic shifts due to boron and hydrogen (Figure 5). These bands are marked by a matrix site splitting to the blue of the main peak. Unlike the other products in the methyl chloride experiments, these bands decrease in intensity upon annealing, then change dramatically upon annealing to 25 K. Similar bands do not appear in the methyl fluoride experiment. The boron isotopic shift is larger for the H products

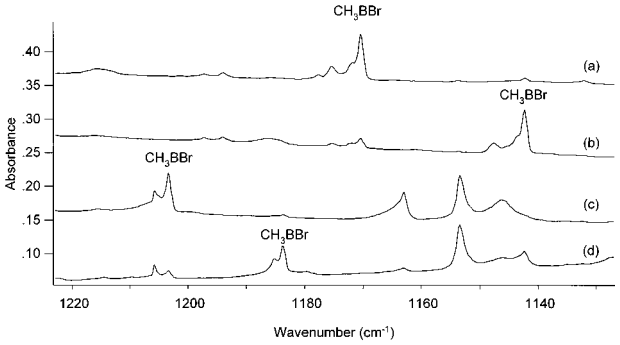

Figure 6. Matrix infrared spectra in the 1225−1125 cm^{-1} B−C stretching region following pulsed laser ablation of B atoms co-deposited with Ar/CH_3Br (200:1) samples on a CsI window at 6−7 K. (a) $^{10}B + CH_3Br$, (b) $^{n}B + CH_3Br$, (c) $^{10}B + CD_3Br$, and (d) $^{n}B + CD_3Br$.

than for the D products, with the deuterated product having a higher frequency in the ^{11}B spectra.

One other band of note appears in the bending region of the spectrum, at 686.9 cm^{-1} for natural isotopes. This absorption has a small boron isotopic shift and larger shift for hydrogen isotopic substitution. This peak tracks with the lower frequency B═C absorption in Figure 4 and may be due to a CH_2 scissors mode, like the 755.0 cm^{-1} peak in the methyl fluoride experiments.

B + CH_2Cl_2 and $CHCl_3$. Supplemental experiments with CH_2Cl_2 and $CHCl_3$ are revealing. The bands in the B═C stretching region both appear in the CH_2Cl_2 experiment, but only the higher energy band appears in the $CHCl_3$ experiment. This indicates that the higher energy B═C absorption belongs to a product with fewer than two hydrogen atoms. Because this absorption also exhibits a deuterium isotopic shift, it must have at least one hydrogen atom. Therefore, this product has a single hydrogen attached. The other B═C vibration appears from a species with two hydrogen atoms. Also notable is the fact that the product absorptions in the 1130−1265 cm^{-1} region of Figure 5 do not appear in either the CH_2Cl_2 or $CHCl_3$ experiments, indicating that this product has three hydrogen atoms.

B + CH_3Br. Results for the methyl bromide experiments closely resemble those of the methyl chloride reactions. Figure 4c shows the B═C stretching region for CH_3Br reactions. As the halogen atom in these products increases in mass, there is a small decrease in the frequencies, indicating a minor role of the halogen in these vibrations. As with the other reactions, there is a large boron isotopic shift with very obvious 1:4 intensity ratios for the $^{10}B/^{11}B$ products in the ^{n}B results (Figure 4). The remainder of Table 2 has the product frequencies observed in the boron−methyl bromide reactions. Also analogous to the other reactions is the smaller deuterium isotopic shift relative to that of boron. The higher and lower frequency bands have indistinguishable photolysis behavior, but the lower frequency band increases on annealing while the higher energy band is unchanged.

The C−H stretching region has accompanying absorptions for the B═C modes. The higher energy stretch, at 3248.2 cm^{-1} for natural isotopes tracks better with the 1665.1 cm^{-1} band, while the lower energy band at 3045.1 cm^{-1} has identical photolysis and annealing behavior to the 1576.0 cm^{-1} peak. These results are entirely consistent with the those of the CH_3F and CH_3Cl experiments.

Figure 6 presents the B−C single bond stretching region of the B/CH_3Br experiments. The absorptions in this region are similar to those of the CH_3Cl reaction products in Figure 5. The boron shift is significant, if smaller than those of the B═C stretching region. Notable is that the deuterated products are of *higher energy* than for natural hydrogen isotopes. This difference is explained in the following section.

Calculations. Table 3 lists the results of BP86 calculations for possible product species in the B (^2P) + $CH_3F(^1A_1)$ reaction. The first two products represent the result of simple insertion into either the B−H or B−F bond on the doublet potential surface. The remainder of the table includes products formed from dehydrogenation following insertion. Although only the most abundant natural isotopic frequencies are listed, it should be noted that deuterated products tend to have weaker absorption intensities and this may be the reason fewer products are observed in the reactions with CD_3F.

Calculations for chloride and bromide products were performed using the same basis sets and BP86 functional. Structures are similar to those of the fluoride products and indicate that only those products with insertion into the boron−halogen bond will be formed based on energy considerations. As shown in the next section, vibrational frequencies predicted from these calculations are generally in excellent agreement with observed data.

Discussion

Identification of products makes use of isotopic shifts in vibrational frequency, involving boron, carbon, and hydrogen, combined with DFT calculations of isotopic frequencies. In natural boron reactions, the ^{10}B and ^{11}B products appear with the 1:4 relative intensities characteristic of single boron atom species.

Species 1: CH_2BF. The B═C stretching modes in Figures 1 and 3 have a very large (approximately 60 cm^{-1}) boron shift and relatively small (approximately 10 cm^{-1}) carbon shift for all isotopic products. Based on the reactions of B with C_2H_6, CH_3NH_2, and CH_3OH, this type of isotopic shift behavior indicates a nearly antisymmetric stretch with boron between carbon and another heavy atom.[1,3,4] In Table 3, three products are given with strong absorptions calculated in this region: CH_2BF, BH_2CF, and CHBF. The first two products are isomers with C_{2v} symmetry, but their calculated energies are very different; CH_2BF is predicted to be 74 kcal/mol more stable than BH_2CF. Also, BH_2CF formation requires C−H bond insertion by the B atom followed by H atom rearrangement. Because no products resulting from C−H bond insertion were observed in the CH_3NH_2 and CH_3OH reactions, this mechanism seems unlikely. Furthermore, the isotopic shifts suggest a B atom vibrating between C and F, which eliminates BH_2CF as a possibility for this peak.

Tables 4 and 5 present the isotopic frequency calculations of CH_2BF and CHBF, as well as their observed frequencies. The B═C stretching frequency of CH_2BF is predicted to be lower than that of CHBF, so the lower bands, labeled product 1, in Figures 1 and 3 belong to CH_2BF. For all isomers, the BP86 calculations are less than 1% higher than the observed frequencies in this region of the spectrum. The boron isotopic frequency ratio for $^{12}CH_2BF$ is observed to be 1.03393, while the calculated ratio is 1.03536, in excellent agreement with experiment. Table 4 shows that the carbon and hydrogen isotopic shifts calculated for this peak are also very close to observed values.

The assignment of the lower frequency band to CH_2BF is further confirmed by comparison to the various chloride reactions. In these experiments, the lower frequency B═C absorption was shown to arise from a product with two hydrogen

TABLE 3: BP86/6-311G* Calculations for Possible Products from Reactions of B with CH_3F

species	energy (a.u.)	bond lengths (Å)	bond angles (degrees)	frequencies in cm^{-1} (intensities in km/mol)[a]
CH_3BF	−164.61910	r_{CH} = 1.11, 1.10; r_{BC} = 1.57; r_{BF} = 1.33	$\angle_{HCB}$ = 113.9, 109.7; $\angle_{HCH}$ = 106.3,108.5; $\angle_{CBF}$ = 122.4	1304.8(179), 254.4(64), 926.8(40)
$^2A'$				
$CH_2(BH)F$	−164.52430	r_{CH} = 1.11; r_{BC} = 1.54; r_{CF} = 1.43; r_{BH} = 1.20	$\angle_{HCB}$ = 110.0; $\angle_{HCF}$ = 107.6; $\angle_{HCH}$ = 105.1; $\angle_{BCF}$ = 115.9; $\angle_{CBH}$ = 133.3	2610.4(64), 1367.1(30), 993.5(35), 876.0(94)
doublet				
CH_2BF[b]	−164.02251	r_{CH} = 1.09; r_{BC} = 1.39; r_{BF} = 1.30	$\angle_{HCB}$ = 121.8; $\angle_{HCH}$ = 116.3; $\angle_{CBF}$ = 180.0	1770.5(373), 764.2(63), 558.5(85)
$^1A_1$				
CH(BH)F	−163.92829	r_{CH} = 1.10; r_{BC} = 1.41; r_{CF} = 1.37; r_{BH} = 1.18	$\angle_{HCB}$ = 120.2; $\angle_{HCF}$ = 12.6; $\angle_{HBC}$ = 174.9; $\angle_{BCF}$ = 127.2;	1183.2(35), 992.1(62), 789.9(39), 661.0(37)
$^1A'$				
BH_2CF	−163.90516	r_{BH} = 1.21; r_{BC} = 1.38; r_{CF} = 1.27	$\angle_{HBC}$ = 118.0; $\angle_{HBH}$ = 124.1; $\angle_{BCF}$ = 180.0	1751.6(297), 848.2(31)
$^1A_1$				
CHBF	−163.35071	r_{CH} = 1.08; r_{BC} = 1.36; r_{BF} = 1.30	$\angle_{HCB}$ = 180.0 $\angle_{CBF}$ = 180.0	3328.9(43), 1854.1(260), 949.9(35), 526.6(35), 93.2(76)
doublet				
BHCF	−163.28250	r_{BH} = 1.18; r_{AC} = 1.35; r_{CF} = 1.29	$\angle_{HBC}$ = 180.0; $\angle_{BCF}$ = 180.0	1851.7(103), 967.7(100)
doublet				

[a] Most abundant isotope, only frequencies with calculated intensities of at least 30 km/mol are shown. [b] A MP2/D95* calculation for $^1A_1$ CH_2BF gave the same bond lengths, a 117.7° HCH angle, and 1835.7(408), 818.2(73), 603.2(100) frequencies (intensities).

TABLE 4: Experimental and Calculated Vibrational Frequencies for CH_2BF in an Argon Matrix for All Observed Absorptions

	$^{11}B/^{12}C/H$	$^{10}B/^{12}C/H$	$^{11}B/^{13}C/H$	$^{10}B/^{13}C/H$	$^{11}B/^{12}C/D$	$^{10}B/^{12}C/D$	$^{10}B/^{11}B$[a]	$^{12}C/^{13}C$[a]	H/D[a]
obsd	3050.2	3050.2	3044.8	3044.8			1.00000	1.00177	
calcd (a_1)	3077.1	3077.3	3070.8	3070.9	2250.9	2253.5	1.00006	1.00205	1.36705
obsd	1762.2	1822.0	1751.3	1816.6	1741.5	1801.0	1.03393	1.00622	1.01189
calcd (a_1)	1770.5	1833.1	1758.8	1822.1	1748.4	1809.0	1.03536	1.00665	1.01264
obsd	917.4	919.5	905.5	905.5			1.00229	1.01314	
calcd (a_1)	899.4	899.7	885.1	885.3	807.4	807.4	1.00033	1.01616	1.11395
obsd	755.0	767.5	748.8	761.4	671.8	687.3	1.01656	1.00828	1.12385
calcd (b_1)	764.2	777.0	757.7	770.6	679.3	695.2	1.01675	1.00858	1.12498
obsd	589.5	590.2	587.0	587.2			1.00119	1.00426	
calcd (b_2)	558.5	559.3	555.4	556.3	430.2	431.9	1.00143	1.00558	1.29884

[a] Isotopic frequency ratio with other isotopes natural.

TABLE 5: Experimental and Calculated Vibrational Frequencies for CHBF in an Argon Matrix for All Observed Absorptions

	$^{11}B/^{12}C/H$	$^{10}B/^{12}C/H$	$^{11}B/^{13}C/H$	$^{10}B/^{13}C/H$	$^{11}B/^{12}C/D$	$^{10}B/^{12}C/D$	$^{10}B/^{11}B$[a]	$^{12}C/^{13}C$[a]	H/D[a]
obsd	3261.7	3261.7	3250.0	3250.0	2468.5	2468.5	1.00000	1.00360	1.32133
calcd	3328.9	3329.4	3315.7	3316.1	2501.8	2506.3	1.00015	1.00398	1.33060
obsd	1822.3	1884.7	1810.8	1872.5	1786.8	1845.3	1.03424	1.00635	1.01987
calcd	1854.1	1918.7	1840.9	1906.3	1807.4	1868.7	1.03484	1.00717	1.02584

[a] Isotopic frequency ratio with other isotopes natural.

atoms, while the higher energy peak correlated with a species with one hydrogen atom.

In further agreement with this assignment are the other bands which track with this product based on photolysis and annealing behavior. The C−H stretch at 3050.2 cm^{-1} is typical of a CH_2 group. The negligible boron isotopic shift and the modest carbon isotopic shift are consistent with this assignment. Further strengthening this assignment is the observation of the B−F "symmetric" stretch at 755 cm^{-1} for natural isotopes. This peak exhibits a boron isotopic shift of 1.01656 (versus 1.01675 predicted), a carbon isotopic ratio of 1.00828 (1.00858), and a hydrogen isotopic ratio of 1.12385 (1.12498). The five fundamental frequencies in Table 4, which agree well with the calculations both in absolute frequency and isotopic shift behavior, provide a high level of confidence for assignment of the ground singlet state ($^1A_1$) CH_2BF molecule. Finally, our calculations predict a bent (C−B−F angle 122°) triplet state some 39 kcal/mol higher at the MP2/D95* level.

Species 2: CHBF. The other B═C stretch belongs to the linear radical CHBF. Table 5 presents the observed and calculated frequencies for this product. Although calculation of radical geometries and frequencies is generally less accurate than for closed shell species, BP86 calculated frequencies are sufficiently close to the observed frequencies to make a definite assignment. Although the calculated results are generally less than 2% higher than their experimental counterparts, the isotopic ratios offer a more revealing indicator of the identity of this species. For the B═C stretch at 1822.3 cm^{-1} (for natural isotopes), the boron isotopic ratio is predicted to be 1.03484, while the observed ratio is 1.03424. Similarly the calculated (observed) carbon isotopic ratio is 1.00717 (1.00635) and the calculated (observed) hydrogen isotopic ratio is 1.02584 (1.01987).

The other band observed for this radical is in the C−H stretching region. The weak band at 3261.7 cm^{-1} is indicative of a CH group. As with CH_2BF, the small boron isotopic shift (within the resolution of the instrument) and moderate carbon

TABLE 6: Experimental and Calculated Vibrational Frequencies for CH_3BCl, CH_2BCl, and CHBCl in an Argon Matrix for All Observed Absorptions

product		$^{11}B/H$	$^{10}B/H$	$^{11}B/D$	$^{10}B/D$	$^{10}B/^{11}B$[a]	H/D[a]
CH_3BCl	obsd	1172.7	1201.2	1161.0	1185.9	1.02430	1.01008
	calcd	1058.3(1289.8)[b]	1091.4(1291.9)	1127.8(1008.3)	1150.8(1010.9)	1.03128	0.93838
CH_2BCl	obsd	-		2232.4	2232.4		
	calcd	3064.3	3064.4	2241.1	2242.9	1.00003	1.36732
	obsd	1605.7	1653.8	1570.3	1625.5	1.02996	1.02254
	calcd	1614.1	1664.8	1582.9	1634.6	1.03141	1.01971
	obsd	686.9	696.0	611.1	623.4	1.01325	1.12404
	calcd	703.3	713.0	611.8	624.2	1.01379	1.14956
CHBCl	obsd	3251.2	3252.3	2464.1	2468.6	1.00034	1.31987
	calcd	3316.7	3317.1	2489.5	2492.8	1.00012	1.33228
	obsd	1691.1	1744.8	1644.3	1696.3	1.03175	1.02846
	calcd	1711.1	1766.5	1658.3	1711.6	1.03238	1.03184

[a] Isotopic frequency ratio with other isotopes natural. [b] Absorption in parentheses "mixed" with major absorption in the region to produce observed band; isotopic ratios use only the major absorption.

isotopic shift are consistent with this assignment. As Table 5 shows, the calculations are in very good agreement with the observed bands. Isotopic shifts are also very close to observed values.

Species 3 and 4: CH_2BCl and CHBCl. Following identification of CH_2BF and CHBF in the boron-methyl fluoride experiments, identification of the chloride analogues is fairly straightforward with further confirmation by experimental and computational evidence. Supported also by the CH_2Cl_2 and $CHCl_3$ experiments, the lower energy peak in Figure 4b is due to CH_2BCl, while the higher energy band arises from CHBCl. The C−H absorptions further confirm these assignments, as the linear ═C−H stretch should have a higher energy than a ═CH_2 vibration, although the latter was only observed in deuterated experiments. The CH_2 scissors vibration in Species 3 further confirms this assignment.

Table 6 presents observed and calculated values for all observed products in the methyl chloride reactions. For CH_2BCl, agreement between experiment and theory is excellent, within 1% for the B═C stretch and 3% for the bending mode. For CHBCl, which has an unpaired electron and is thus less amenable to accurate calculations, both B═C stretches and C−H absorption frequencies are still within 2% of their observed values. Calculated boron and hydrogen isotopic ratio shifts are also in excellent agreement with experiment. In both these products, the B═C vibration is calculated to be by far the strongest, as observed, and resembles an antisymmetric mode, giving rise to the large boron isotopic shift.

Species 5: CH_3BCl. Unlike the methyl fluoride reactions, new product bands appear in the B−C stretching region of the spectrum in the chloride experiments. Because these products do not appear in the CH_2Cl_2 and $CHCl_3$ reactions, it is possible that the product giving rise to the bands in Figure 5 possesses three H atoms. These bands do not appear in experiments without chlorine, indicating that they have a Cl atom. On the basis of these observations, this absorption is assigned to the primary insertion product, CH_3BCl.

Table 6 presents calculations for this product for comparison to the observed values. Note that the calculations are not as accurate as for CH_3BCl. Part of the reason may be the unpaired electron on the boron, which makes accurate calculation of vibrational frequencies difficult, but another factor may be mixing between two modes to produce the observed results. When two bands of similar symmetry are of comparable frequency, they perturb each other and cause an energy shift. If calculations are inaccurate, the further shifting due to this perturbation will also be inaccurate. As Table 6 shows, there are two bands calculated generally within 250 cm^{-1} of each other, enabling some weak perturbation. Also, the small deuterium shift (positive for ^{10}B products) is a result of the lower energy absorption possessing the larger oscillator strength for CH_3BCl, while the higher energy absorption dominates for CD_3BCl.

Species 6−8: CH_2BBr, CHBBr, and CH_3BBr. Comparison of the CH_3Br reactions with the CH_3F and, especially, the CH_3Cl reactions, enables clear identification of three new products. The lower energy B═C stretch, at 1576.0 cm^{-1} for natural isotopes, arises from CH_2BBr, while the 1665.1 cm^{-1} peak is assigned to CHBBr. The C−H stretches are similar, with the CHBBr absorption appearing approximately 200 cm^{-1} higher in energy than that of CH_2BBr. Although no lower energy bands were observed, the appearance of these bands in the signature regions enables positive identification of the three products. As Table 7 shows, agreement between observed and calculated frequencies is excellent, with less than 1% disparity for the closed-shell CH_2BBr product.

Similar to the process for CH_3BCl, identification of CH_3BBr is complicated by unusual deuterium isotopic shifts, in this case positive for both isotopes of boron. The calculations predict this positive shift, as the relative oscillator strengths of nearly isoenergetic modes shift upon deuteration. Agreement between experiment and computation is very good for CD_3BBr, but CH_3BBr is apparently affected more by mode mixing. Nevertheless, because of the comparison with the methyl chloride experiments, the assignment of CH_3BBr is straightforward.

Comparison with Other Reactions. The major pathways in previous reactions involved insertion as follows:

$$B + CH_3CH_3 \rightarrow [CH_3{-}B{-}CH_3]^* \rightarrow CH_3BCH_2 + H$$

$$B + CH_3NH_2 \rightarrow [CH_3{-}B{-}NH_2]^* \rightarrow CH_3BNH + H$$

$$B + CH_3OH \rightarrow [CH_3{-}B{-}OH]^* \rightarrow CH_3BO + H$$

In none of these cases was the intermediate product observed (e.g., no observed CH_3BOH). For the methyl fluoride reaction, insertion into the B−F bond occurs as follows:

$$B{+}CH_3F \rightarrow [CH_3{-}B{-}F]^* \rightarrow CH_2BF + H \text{ and } CHBF + H_2$$

As with the previous reactions, in this reaction there is no observed CH_3BF. In all cases, loss of hydrogen followed insertion. Also, there were no observed products arising from

TABLE 7: Experimental and Calculated Vibrational Frequencies for CH_3BBr, CH_2BBr, and CHBBr in an Argon Matrix for All Observed Absorptions

product		$^{11}B/H$	$^{10}B/H$	$^{11}B/D$	$^{10}B/D$	$^{10}B/^{11}B$[a]	H/D[a]
CH_3BBr	obsd	1142.4	1170.5	1161.0	1185.9	1.02460	0.98398
	calcd	1033.4(1288.6)[b]	1064.6(1290.4)	1117.6(1004.9)	1137.2(1006.8)	1.03019	0.92466
CH_2BBr	obsd	3045.1	3045.1	2224.7	2227.2	1.00000	1.36877
	calcd	3063.0	3063.1	2239.3	2240.9	1.00003	1.36784
	obsd	1576.0	1620.7	1541.0	1586.6	1.02836	1.02271
	calcd	1579.7	1626.8	1546.9	1595.1	1.02982	1.02120
CHBBr	obsd	3248.2	3250.4	2461.9	2465.1	1.00068	1.31939
	calcd	3313.5	3313.9	2486.1	2489.3	1.00012	1.33281
	obsd	1665.1	1716.6	1616.3	1666.3	1.03093	1.03019
	calcd	1679.0	1731.8	1625.1	1676.2	1.03145	1.03317

[a] Isotopic frequency ratio with other isotopes natural. [b] Absorption in parentheses "mixed" with major absorption in the region to produce observed band; isotopic ratios use only the major absorption.

C−H insertion. As Table 3 demonstrates, these products are generally much less stable than the isomers observed. In the CH_3NH_2 and CH_3OH reactions, there was insertion into the C−N and C−O bond followed by loss of H from the C atom, but these products, CH_2BNH_2 and CH_2BOH, were less abundant than the main species.[3,4] In the C_2H_6 reaction, such a product, CH_2BCH_3 is actually the same as the main product,[1] and this reaction is therefore not a comparable situation. In all of these reactions, however, other products resulting from more hydrogen loss from the intermediate were present in the matrix. Based on these previous reactions then, it is reasonable to conclude that CH_2BF and CHBF are the only products formed by an insertion reaction, and the lack of observation of other products results from the very limited pathways for reaction.

One difference in the products of the methyl fluoride reaction compared to the ethane, monomethylamine, and methanol reactions is the lack of a formal charge on the fluorine. In CH_3BCH_2, carbon has no lone pair to donate to the boron empty p-orbital, but in CH_3BNH and CH_3BO, the nitrogen and oxygen, respectively, do such a thing, thereby shortening the expected B−N and B−O bonds.[3,4] As Table 3 shows, the B−F distance calculated in CH_2BF and CHBF, 1.30 Å, is only slightly shorter than that of the single bond calculated in CH_3BF, 1.33 Å. This would suggest that the lone pairs of fluorine do not interact with the boron atom in the bonding of these product species.

Conclusions

The reaction of laser-ablated boron atoms with methyl fluoride yields two new products, CH_2BF and CHBF, which are isolated in an argon matrix. Similar reactions with methyl chloride and methyl bromide also yield CH_2BX and CHBX, but also CH_3BX. The mechanism of formation involves insertion into the C−X bond, and not the C−H bonds, followed by loss of one or two H atoms. BP86/6-311G* calculations for the methyl fluoride reactions show that the reaction products resulting from this mechanism are far more energetically stable than other isomers. No CH_3BF primary insertion intermediate was detected in the matrix, but this product appears in the CH_3Cl and CH_3Br experiments. Compared to the previously studied reactions of B with C_2H_6, CH_3NH_2, and CH_3OH, in this laboratory,[1,3,4] there are fewer possible reaction products. In the previous reactions, the major product resulted from insertion between heavy atoms followed by H loss from the more electronegative heavy atom. Because in this CH_3F experiment, the F atom is terminal, no such mechanism is possible. Also notable is that, although the isoelectronic molecules CH_2BNH_2 and CH_2BOH have near double-bond character in the B−N and B−O bonds, the B−F bond in CH_2BF is very much a single bond.

Acknowledgment. This work was supported by the Air Force Office of Scientific Research. Calculations were performed on the University of Virginia SP2 machine.

References and Notes

(1) Andrews, L.; Lanzisera, D. V.; Hassanzadeh, P.; Hannachi, Y. *J. Phys. Chem. A* **1998**, *102*, 3259.

(2) Hassanzadeh, P.; Hannachi, Y.; Andrews, L. *J. Phys. Chem.* **1993**, *97*, 6418.

(3) Lanzisera, D. V.; Andrews, L. *J. Phys. Chem. A* **1997**, *101*, 824.

(4) Lanzisera, D. V.; Andrews, L. *J. Phys. Chem. A* **1997**, *101*, 1482.

(5) Burkholder, T. R.; Andrews, L *J. Chem. Phys.* **1991**, *95*, 8697.

(6) Hassanzadeh, P.; Andrews, L. *J. Phys. Chem.* **1992**, *96*, 9177.

(7) Thompson, C. A.; Andrews, L.; Martin, J. M. L.; El-Yazal, J. *J. Phys. Chem.* **1995**, *99*, 13839.

(8) Frisch, M. J.; Trucks, G. W.; Schlegel, H. B.; Gill, P. M. W.; Johnson, B. G.; Robb, M. A.; Cheeseman, J. R.; Keith, T.; Petersson, G. A.; Montgomery, J. A.; Raghavachari, K.; Al-Laham, M. A.; Zakrzewski, V. G.; Ortiz, J. V.; Foresman, J. B.; Cioslowski, J.; Stefanov, B. B.; Nanayakkara, A.; Challacombe, M.; Peng, C. Y.; Ayala, P. Y.; Chen, W.; Wong, M. W.; Andres, J. L.; Replogle, E. S.; Gomperts, R.; Martin, R. L.; Fox, D. J.; Binkley, J. S.; Defrees, D. J.; Baker, J.; Stewart, J. P.; Head-Gordon, M.; Gonzalez, C.; Pople, J. A. *Gaussian 94, Revision B.1;* Gaussian, Inc.; Pittsburgh, PA, 1995.

(9) Becke, A. D. *Phys. Rev.* **1988**, *38*, 3098; Perdew, J. P. *Phys. Rev. B* **1986**, *33*, 8822.

(10) McLean, A. D.; Chandler, G. S. *J. Chem. Phys.* **1980**, *72*, 5639. Krishnan, R.; Binkley, J. S.; Seegar, R.; Pople, J. A. *J. Chem. Phys.* **1980**, *72*, 650.

(11) Lanzisera, D. V.; Andrews, L. *J. Am. Chem. Soc.* **1997**, *119*, 6392.

(12) Zhou, M. F.; Andrews, L. *J. Am. Chem. Soc.* **1998**, *120*, 11499.

(13) Zhou, M. F.; Andrews, L. *J. Chem. Phys.* **1999**, *100*, 10370.

(14) Zhou, M. F.; Andrews, L. *J. Phys. Chem. A* **1999**, *103*, 6956 and 7773.

(15) Lanzisera, D. V.; Andrews, L. To be published.